Int. J. Multiphase Flow Vol. 19, No. 1, pp. 35–49, 1993
Printed in Great Britain.

0301-9322/93 $6.00 + 0.00

THE RELATION BETWEEN THE INTERFACIAL SHEAR STRESS AND THE WAVE MOTION IN A STRATIFIED FLOW

H. C. KANG[1] and M. H. KIM[2]

[1]Department of Mechanical Design, Kunsan National University, Kunsan 573-360, South Korea

[2]Department of Mechanical Engineering, Pohang Institute of Science and Technology, P.O. Box 125, Pohang 790-600, South Korea

(Received 18 June 1991; in revised form 30 August 1992)

Abstract—A model is developed to describe the interfacial shear stress at a wavy interface with wave characteristics. Experiments have been conducted with near-horizontal (4.1°) and near-vertical (87°) flat plates for air–water concurrent stratified flows. The interfacial shear stress and normal and flow directional interface velocities were measured. Assuming a simple relation between the gas velocity near the interface and film thickness, the turbulent shear stress due to the wave motion is expressed by the normal interfacial velocity and the relative gas velocity. The model developed agrees well with the experimental data for a wide range of horizontal and vertical stratified flow.

Key Words: waves, interfacial shear stress, wave velocities, gas–liquid flows, film thickness, turbulent shear stress, stratified flow, conductance probe

1. INTRODUCTION

Interfacial shear stress is a major factor governing transport processes, such as heat and mass transfer, in a stratified flow. Many studies have been performed to elucidate the effect of interfacial structures on this process from various points of view.

The work by Lockhart & Martinelli (1949) was one of the earliest analytical studies to predict the pressure drop in a gas–liquid flow. Although this attempt may have been the simplest one, and was applicable to all kinds of flow regimes, the accuracy was not sufficient. Wallis (1969) suggested a simple correlation between the film thickness and the interfacial friction factor based on experimental data in a vertical annular flow. Lilleleht & Hanratty (1961) correlated the interfacial shear stress with Nikuradse's measurement with sand roughness. Hanstock & Hanratty (1976) summarized the experimental data and recommended equations to estimate the friction factors in annular flows. A factor which characterizes the flow condition was introduced to eliminate the dependence of the film thickness on the interfacial shear stress. All these works made great contributions to applications. The wavy interface was, however, treated as a rough wall surface having the same interfacial shear stress, without considering wave motion. Fukano *et al.* (1985) compared the interfacial stress data of horizontal stratified flow with previous models. They concluded that the stress depends on the flow regime, and it is very hard to treat the wavy interface as a rough wall surface for all flow regimes. Chu & Dukler (1974, 1975) classified film waves into large and small. They calculated the form drag due to the large waves from the local pressure and film thickness data, and concluded that the primary contribution to the increase in shear in annular flow is from the small waves. But the role of the small waves in the transport process was not clarified. Some work has been done on the characteristics of the gas velocity close to the interface. Pioneering work was done by Chang *et al.* (1971) from a microscopic point of view. Their experimental data showed that the velocity of the gas close to the interface was strongly affected by the interface's shape, and the turbulent energy spectrum of the gas velocity had dominant power at the frequency of the dominant wave. Akai *et al.* (1977) conducted a similar experiment on an air–water stratified flow. They measured the turbulent shear stress, which is greatly enhanced in the wavy interface. Hagiwara *et al.* (1989) simultaneously measured the wall shear stress, liquid film thickness and streamwise gas velocity with a hot-film probe in a horizontal tube. They observed that the large wave causes an increase in the wall shear stress. Various workers have declared, with

no clear explanation, that shear stress and turbulent characteristics are increased in a wavy interface.

What enhances the shear stress in the wavy interface? The previous models say that the shear stress in a wavy interface is different from that on a rough wall surface with the same roughness as the wave amplitude. If so, the answer to the question may be what is different from the rough wall surface. In fact, the wavy interface generates a continuously varying interface motion which is different from the solid wall surface. The interface motion changes the gas flow. Unfortunately, it is not easy to measure gas velocities in an interface region affected by wavy motion. One way to explain the transport phenomena in the interface is the use of well-balanced film thickness data.

In this paper, a new model is developed to correlate the momentum transfer in the wavy interface with the wave and gas velocities. The model is then compared with experimental data for the horizontal and vertical stratified flow on a flat plate.

2. EXPERIMENT

The experimental facility is designed to measure the film thickness, the gas velocity and the pressure drop in the air–water concurrent stratified flow, as shown in figure 1. The test section is made of an acrylic resin duct, 170 cm long, 5 cm high (H) and 15 cm wide (W). Air is fed into the test section though the honeycomb and screen to enhance the flow quality. The water from the reservoir tank is supplied to the test section through the water injection system. A 25 cm free-running section is provided to maintain uniformity at the water injector. A constant water flow rate is maintained to within 1% using a constant head tank. The inclination of the test section is changed by the hinge located at its center. Two inclinations were used for the test section; nearly horizontal (4.1°), and nearly vertical (87°). Recently, Kang & Kim (1992a) investigated the geometry of conductance probes for measuring liquid film thickness, and concluded that the flush-wire probe has better spatial resolution than typical conductance probes, i.e. flush-mounted and parallel-wire probes. In this work, two flush-wire probes separated by a distance along the flow direction are used to measure film thicknesses simultaneously, as shown in figure 2. Platinum wires, 0.05 mm dia, are used as measuring electrodes to minimize the flow disturbance and distortion of the interface. The spatial and temporal resolutions of the probes are far finer than the film thickness and wave frequency. The probes are calibrated using the probability of the existence of liquid, as

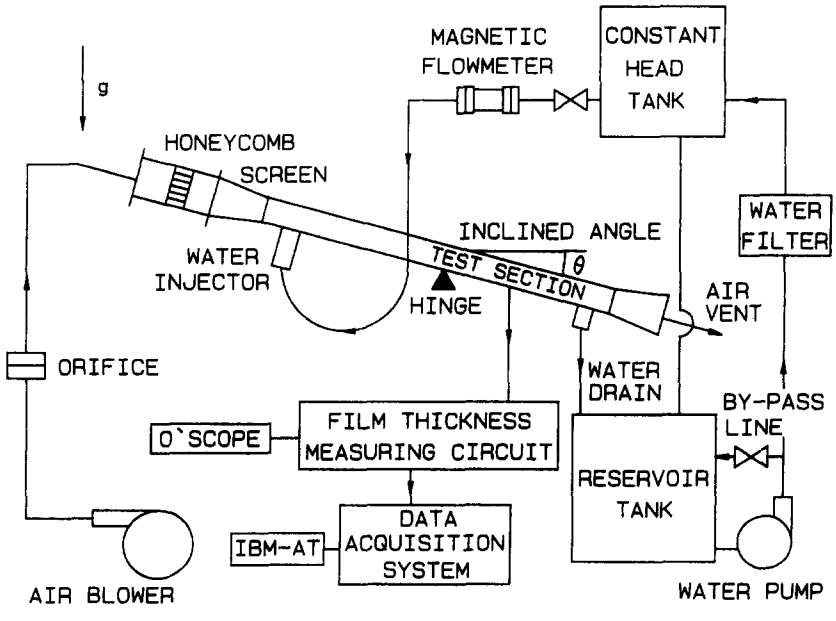

Figure 1. Schematic diagram of the experimental setup.

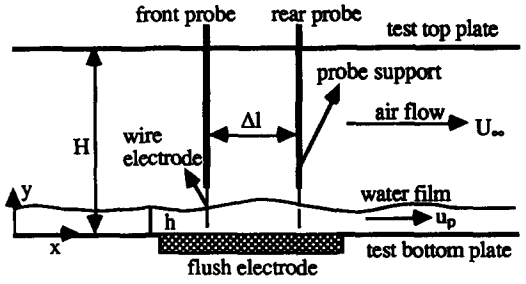

Figure 2. Two flush-wire probes for the simultaneous measurement of the water film thickness.

described by Kang & Kim (1992a). Figure 3(a) shows a typical example of film thickness traces from the front and rear probes. The air velocity and air flow rate are measured by a Pitot tube and micro-manometer system and an orifice flowmeter. The pressure drop is measured by another micro-manometer which has 2 mm H_2O in its full scale at the top side of the test section. The

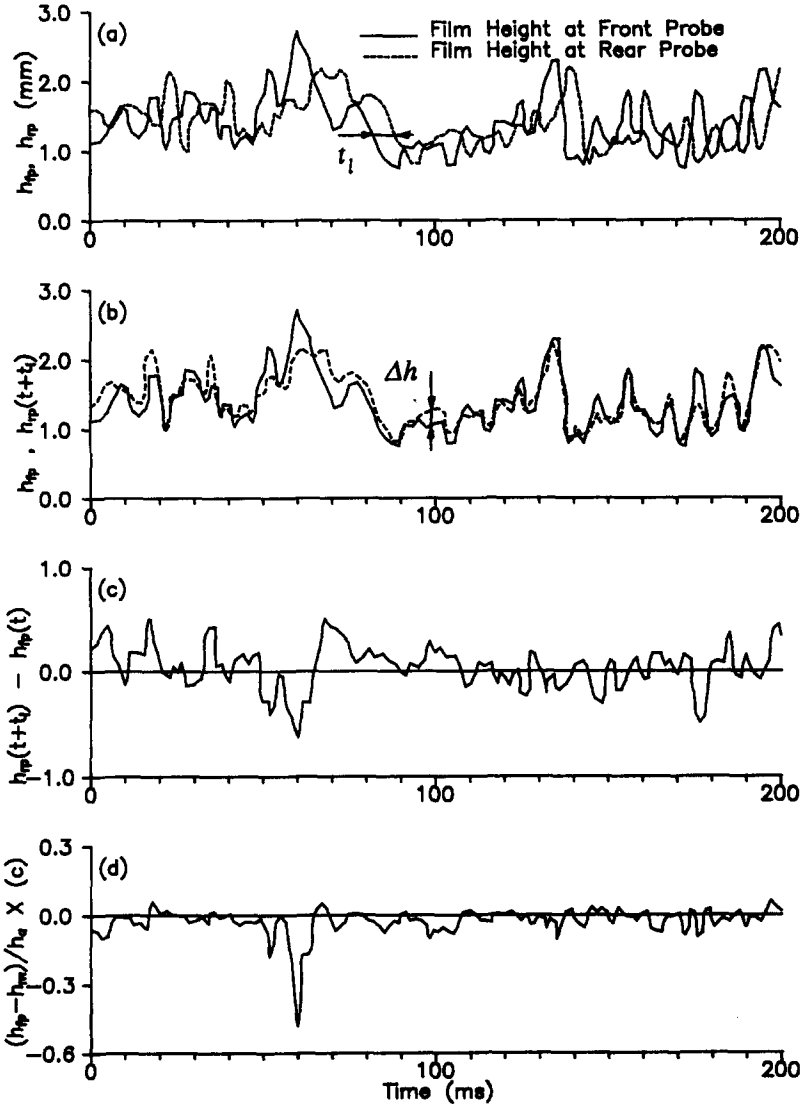

Figure 3. Typical example of film thickness traces and their correlation (case, $\theta = 4.1°$, $Re_L = 998$, $U_\infty = 10$ m/s, $\Delta l = 5$ mm): (a) film thickness traces at the front and rear probes; (b) variation of the film height when the rear film height is shifted by a time lag; (c) displacement of the front film height during the time lag; (d) correlation between the front film height and the displacement in (c).

Table 1. Experimental conditions

Condition	Unit	Horizontal film	Vertical film
Inclined angle (θ)	deg	4.1	87
Water flow rate (Q_L)	m^2/s	4.44×10^{-4}–1.11×10^{-3}	
Air velocity (U_∞)	m/s	0–10	0–12
Sample rate ($1/\Delta t$)			
(calibration)	No./s	150	200
(wave velocity)	No./s	1000	1000
Distance of front and rear probe (Δl)	mm	5	25

distance between the pressure taps is 20 cm. The water flow rate is measured by a magnetic flowmeter (OMEGA type FMG-11). The film thickness and air velocity are measured 132 cm downstream from the water inlet. The characteristics of the film are not sufficiently fully developed at the measuring location, but the statistical properties of the wave are nearly constant, as discussed by Portalski & Clegg (1972) and Salazar & Marschall (1978). A detailed description of the test apparatus and the measuring technique is given in Kang & Kim (1992a). The experimental conditions are listed in table 1. All experiments were performed at atmospheric pressure, at $25 \pm 1°C$.

The shear stress is calculated by a momentum balance method, similar to that described by Kowalski (1987). If the momentum change of the air along the flow direction is negligible, the force balance in the test section is

$$W \cdot (H - h_m) \cdot \Delta P = L \cdot [2(H - h_m) + W] \cdot \tau_{sw}(U_\infty) + L \cdot W \cdot \tau_i(U_\infty), \quad [1]$$

where W, H, L, h_m and ΔP are the test section width and height, the distance between the pressure taps, the mean film thickness and the pressure drop, respectively. The quantities $\tau_{sw}(U_\infty)$ and $\tau_i(U_\infty)$ are the shear stress on the smooth wall surface and the interfacial shear stress with maximum air velocity U_∞ at the core of the test section. Throughout this paper the interface velocity components are denoted by u and v for the flow direction and the direction normal to the wall, and the gas velocity components are denoted by U and V for the corresponding directions. The interfacial shear stress is then expressed as follows:

$$\tau_i(U_\infty) = \frac{H - h_m}{L} \cdot \Delta P - \frac{2(H - h_m) + W}{W} \cdot \tau_{sw}(U_\infty). \quad [2]$$

The wall shear stress $\tau_{sw}(U_\infty)$ is influenced by the test geometry and the inlet condition. Its measured value is slightly larger than the calculated value for a flat plate, as shown in figure 4. This may be partly due to the flow at the corner of the channel and the inlet conditions. The discrepancy

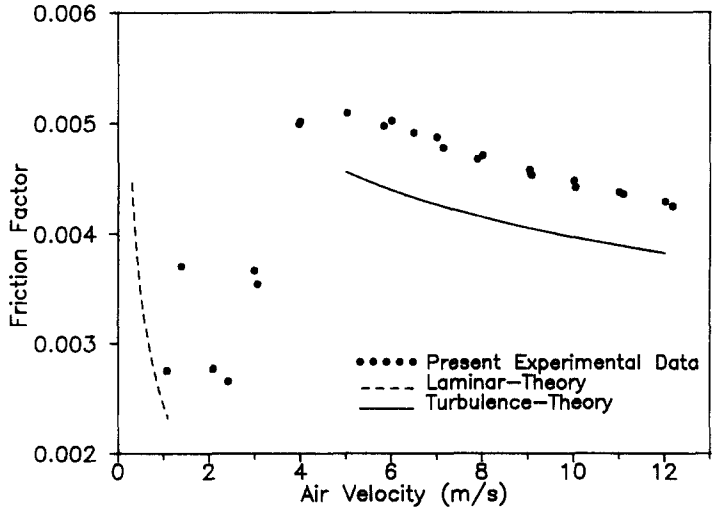

Figure 4. Comparison of the measured wall shear stress with the theoretical value.

between the measured shear stress and the theoretical value on the smooth wall surface is small and in the same direction. However, we used the measured $\tau_{sw}(U_\infty)$ to calculate the interfacial shear stress $\tau_i(U_\infty)$, to maintain consistency.

3. WAVE VELOCITIES

The wave motion is a very complex one to understand, but the wave velocity is very important in the explanation of the interaction between the air and water. The definition of the coordinate system used to explain the wave motion is described in figure 5. The interface shape h related to the interfacial shear stress is a function of the flow directional coordinate x and time t, and is expressed as follows:

$$h = f(x, t). \quad [3]$$

Let us first discuss the flow directional wave velocity of the interface u. The total wave velocity in the flow direction, denoted by u_c, is decomposed into the film velocity on the interface u_p and the wave propagation velocity u_w, as shown in figure 5(a), and is expressed as follows:

$$u_c = u_p + u_w. \quad [4]$$

The total wave velocity u_c can be calculated by the cross-correlation R of the film thickness at the front and rear probes. It is written as follows:

$$R_{h_{fp}h_{rp}}(j) = \frac{1}{n}\sum_{i}^{n} h_{fp}(i)h_{rp}(i+j), \quad [5]$$

$$t_l = (R_{h_{fp}h_{rp}}(j))_{max}\,\Delta t \quad [6]$$

and

$$u_c = \frac{\Delta l}{t_l}, \quad [7]$$

where the subscripts "fp" and "rp" denote the front and rear probe. The notation i, j and n are the datum number and the total number of data, and Δt and Δl are the measuring time step and the distance between the two probes, respectively, as described in table 1.

The film velocity on the interface u_p arises due to the bulk flow of liquid. For large film Reynolds number, the velocity profile in the liquid film can be assumed to be given by the wall function of

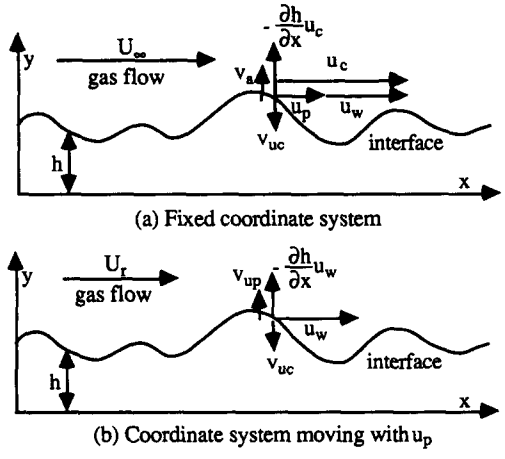

Figure 5. Definition of the coordinate systems to explain the interface velocities.

the turbulent flow on the flat plate. Similarly to Levy & Healzer (1981) and Kim (1983), the velocity on the interface is expressed using Prandtl mixing length theory as follows:

$$u_p = u_L + 2\sqrt{A - By} + \sqrt{A} \cdot \ln\left(\frac{\sqrt{A - Bh_m} - \sqrt{A}}{\sqrt{A - Bh_m} + \sqrt{A}}\right) - 2\sqrt{A - By_l} - \sqrt{A} \cdot \ln\left(\frac{\sqrt{A - By_l} - \sqrt{A}}{\sqrt{A - By_l} + \sqrt{A}}\right), \quad [8]$$

where

$$u_L = \frac{g \sin\theta}{\nu_L} \cdot (h_m y_l - \tfrac{1}{2} y_l^2) + \frac{\rho_L \tau_i y_l}{\nu_L},$$

$$y_l = \frac{11.6\nu_L}{\sqrt{\frac{\tau_i + \rho_L g \sin\theta}{\rho_L}}},$$

$$A = 6.25\frac{\tau_i}{\rho_L} + Bh_m$$

and

$$B = 6.25 g \sin\theta.$$

In the above equation, y_l is the thickness of the viscous sublayer and u_L is the liquid velocity at y_l.

The interface velocity component normal to the wall v is related to the variation of the film thickness h. The normal velocity at the fixed point is the time variation of the film thickness measured at the location of the flush-wire probe. It can be expressed by the central difference method as follows:

$$v_a = \left(\frac{dh}{dt}\right) = \frac{h(i + \frac{1}{2}) - h(i - \frac{1}{2})}{\Delta t}. \quad [9]$$

The velocity v_a is the summation of the convected variation due to the interface slope $\partial h/\partial x$ and the normal directional time variation of the interface v_{uc}, as shown in figure 5(a):

$$v_a = -u_c \frac{\partial h}{\partial x} + v_{uc}. \quad [10]$$

The velocity v_{uc} is the normal directional velocity component due to the change in the wave shape. If the wave is monochromatic, v_{uc} should be zero. For a general stratified flow, the interface is formed by multi-component waves which have different wave shapes and velocities. The velocity v_{uc} means the normal directional deformation velocity seen by an observer who follows the wave with the total wave velocity u_c. A wave that touches the front probe will touch the rear probe after time t_l of [6]. If the interface measured at the rear probe is shifted as much as the t_l, the difference in the two film heights Δh is the change in the interface during the time t_l. A typical example is shown in figures 3(a–c). The velocity v_{uc} and the change in thickness of the interface Δh during the time t_l, are expressed as

$$\Delta h = h_{rp}(i + R_{h_{fp}h_{rp}}(j)_{max}) - h_{fp}(i) \quad [11a]$$

and

$$v_{uc} = \frac{\Delta h}{t_l}. \quad [11b]$$

The v_{uc} is caused by the small wave components. When the interface with the superimposed multi-component waves is located at a maximum wave crest, the interface can only move downward, in view of the flow directional velocity u_c. When the interface is located at a minimum trough, the reverse holds. In other words, v_{uc} is statistically negative at a crest, and positive at a

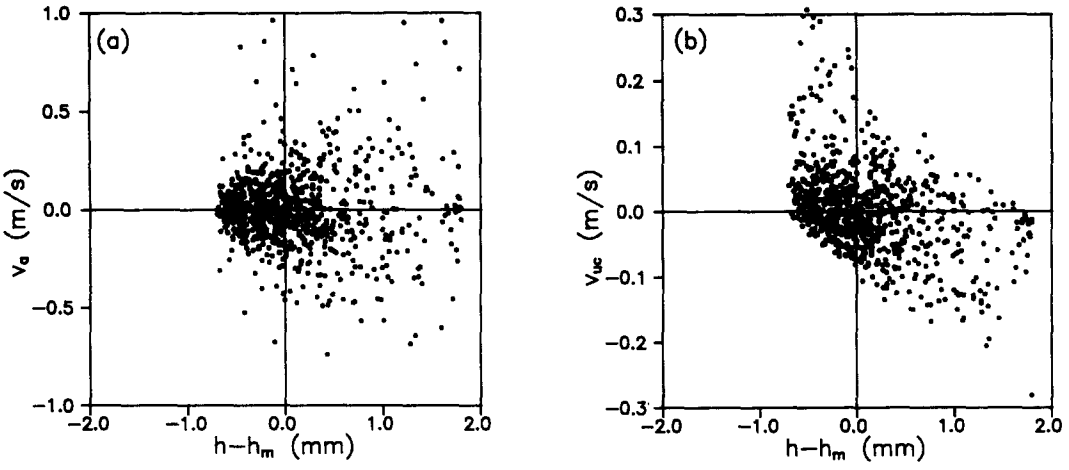

Figure 6. Correlations between the film thickness and: (a) the normal velocity at a fixed point [correlation coefficient $\rho_{(h-h_m),v_a} = 0.0$]; (b) the normal velocity at the coordinate moving with interface velocity u_p [correlation coefficient $\rho_{h-h_m),v_{uc}} = -0.401$]. (Case, $\theta = 87°$, $Re_L = 998$, $U_\infty = 6$ m/s.)

trough. This is clearly shown in figure 6(b), which plots the normal interface velocity v_{uc} along the film thickness $(h - h_m)$. Therefore, v_{uc} has a negative correlation with the liquid film thickness. This gives an important clue to the shear stress caused by the wave motion. In the calculation of v_{uc}, the flow directional velocity u_c is not exactly constant. It is very hard to describe reasonably the fluctuation of the flow directional velocity of a wave, it is assumed constant in this work.

The normal directional wave velocity, in view of the moving coordinate system with the interface velocity u_p, is expressed similarly to [10]:

$$v_{up} = -u_w \frac{\partial h}{\partial x} + v_{uc}. \qquad [12]$$

The interface slope $\partial h/\partial x$ of [12], which governs the interface shape, is conserved in any coordinate system. The normal direction time-varying velocity v_{uc} is unchanged for a flow directional coordinated system, since v_{uc} is independent of the flow directional velocity. Using [4] and [10], [12] can be rewritten using measurable velocities:

$$v_{up} = \frac{u_w}{u_c} v_a + \frac{u_p}{u_c} v_{uc}. \qquad [13]$$

The need for the velocity component v_{up} will be explained in the next section.

4. MODELING OF INTERFACIAL SHEAR STRESS

Some previous researchers have tried to correlate the interfacial shear stress with a rough wall surface having the same shear stress. Fukano *et al.* (1985) compared the interfacial shear stress with Schlichting's (1962) measurement of the wall shear stress on a flat plate having three types of protrusion. The characteristics of an interface are, however, very different from those of a rough wall surface. Portalski & Clegg (1971) measured the increase in interfacial area by the photographic method. They concluded that the increase in interfacial area is $<1\%$ for vertical film up to $Re_L = 750$. Hereafter Re_L is defined by Q_L/ν_L, where Q_L and ν_L are the volume flow rate per unit width and the kinematic viscosity of the liquid. Recently, Kang & Kim (1992b) measured the three-dimensional wave shape and the interface area using a multi-conductance probe in a horizontal and vertical stratified flows. The typical ratio of wave amplitude to the wavelength is about 10%. The ratio of the interfacial area to its base area is also less than a few percent in the experimental range of table 1. Karapantsios & Karabelas (1990) have conducted experiments on the roll wave of a free-falling film in a vertical pipe. They state that the average slope of a wave's front is about twice that of its back. Even the larger slope is, however, small; about 20° up to $Re_L = 3250$. From these results, it seems unreasonable to

correlate the interfacial wave characteristics with the sand roughness. Moreover, the wavy interface is supposed to be a smooth wall surface rather than a rough wall surface.

Chang *et al.* (1971) noted that the turbulent energy spectrum of the gas velocity has its largest value near the dominant wave frequency, and the trend of the spectrum at frequencies higher than this remains unaltered along the distance from the interface. From these results, the interfacial shear stress is thought to be composed of the shear stress on the rigid wall surface and the turbulent shear stress due to the wave motion.

Since the interface moves with the velocity u_p, discussed in the previous section, it is reasonable to describe the shear stresses and gas velocities in terms of the moving coordinate system u_p. The interfacial shear stress can be expressed as the sum of the shear stress on a rigid surface of the same shape as the wavy interface $\tau_{fs}(U_r)$ and the turbulent shear stress by moving interface $\tilde{\tau}(U_r)$:

$$\tau_i(U_\infty) = \tau_{fs}(U_r) + \tilde{\tau}(U_r) \quad [14]$$

and

$$U_r = U_\infty - u_p, \quad [15]$$

where both shear stresses should be calculated based on the relative gas velocity U_r. The area of the wavy interface is larger than its base area, so this should be considered. The shear stress exerted on a rigid surface of the same shape as the wavy interface is expressed as

$$\tau_{fs}(U_r) = \gamma \tau_{sw}(U_r), \quad [16]$$

where $\tau_{sw}(U_r)$ is the shear stress exerted on the smooth wall surface with the relative gas velocity U_r and γ is a factor that represents the contribution of the increased surface area. The turbulent stress $\tilde{\tau}(U_r)$ can be expressed as the gas velocity fluctuations $\tilde{V}$ and $\tilde{U}$ by the wave motion as follows:

$$\tilde{\tau}(U_r) = (-\rho_G \overline{\tilde{U} \cdot \tilde{V}})_{up}. \quad [17]$$

The normal directional gas velocity $\tilde{V}$ close to the interface may be nearly the same as the normal interface velocity in this moving coordinate system:

$$\tilde{V} \cong v_{up}$$

$$= \frac{u_w}{u_c} v_a + \frac{u_p}{u_c} v_{uc}. \quad [18]$$

It is very hard to predict the flow directional gas velocity $\tilde{U}$ in the interface region. It will be affected by numerous variables, such as wave height, wavelength, gas velocity, gas properties and the interfacial velocities. The measured data of Chang *et al.* (1971) show that the bulk gas flow close to the interface is very similar to the wave shape. The streamline pattern plotted from the experimental data follows the wave shape with some separation regions behind the wave crests. Most of the wave effects on the gas flow reached up to one wave amplitude from the wave crests. Therefore, the flow directional gas velocity U_r is assumed to be greatly affected by the wave shape or the film height. If an interface Reynolds number ($Re_i = U_r h_a / \nu_G$) is defined by the gas velocity U_r and the maximum wave amplitude h_a, the values of Chang *et al.* ($Re_i \sim 12{,}000$, $h_a \sim 24$ mm and $U_r \sim 8$ m/s) are 10 times larger than those in the present cases ($Re_i \sim 1100$, $h_a \sim 2$ mm and $U_r \sim 10$ m/s). The effect may grow in high gas velocity and thick film ranges. The value of Re_i may be smaller than that of Chang *et al.* for thin film flow. Akai *et al.* (1977) performed a similar experiment with horizontal stratified flow and observed the effective depth—defined as the distance from the wave crests to the points where no periodic effect could be observed. They report that the effective depth seems to be nearly equal to the wave amplitude. Their results are similar to those of Chang *et al.* (1971).

From these results the bulk gas velocity will take its maximum value at the wave crest [figure 7(a)] and minimum value at the trough [figure 7(b)]. Then the fluctuating gas velocity $\tilde{U}$ can be assumed to be dependent on the relative gas velocity U_r, the wave height h and the wave amplitude

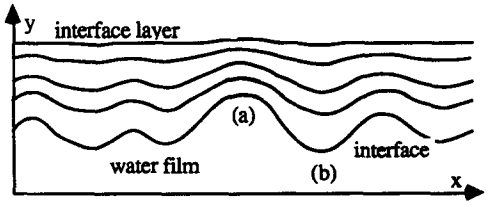

Figure 7. Interface layer region and the assumed streamline close to the interface.

h_a. If we assume that the relation is simply linear in the film thickness without flow separation, the fluctuating gas velocity near the interface is represented by

$$\tilde{U} = c_1 \cdot U_r \frac{h - h_m}{h_a}. \quad [19]$$

The shear stress from the wave motion of [17] can be deduced from [18] and [19]:

$$(-\rho_G \overline{\tilde{U} \cdot \tilde{V}})_{up} = -c_1 \frac{\rho_G U_r}{h_a} \overline{(h - h_m) \cdot \left(\frac{u_w}{u_c} v_a + \frac{u_p}{u_c} v_{uc} \right)}. \quad [20]$$

The first term on the RHS must be zero in fully developed stratified flow, since there is no correlation between the film thickness and the normal interface velocity in the fixed coordinate system. If there is some correlation, then the mean film thickness must increase or decrease. This agrees with the results of figure 6(a), which plots the normal interface velocity measured at a fixed point along the film thickness $(h - h_m)$. The shear stress due to the wave motion of [20] is

$$(-\rho_G \overline{\tilde{U} \cdot \tilde{V}})_{up} = -c_1 \frac{\rho_G U_r u_p}{h_a u_c} \overline{(h - h_m) \cdot v_{uc}}, \quad [21]$$

where $(h - h_m)$ and v_{uc} have a negative correlation, shown in figure 3(d) and figure 6(b) which plots the normal interface velocity measured with moving u_c along the film height. If $(h - h_m)$ and v_{uc} are assumed to be correlated with some factor c_2, then a new coefficient c is defined as

$$c = c_1 c_2. \quad [22]$$

The coefficient c is negative, since c_1 and c_2 are positive and negative. Then [21] can be simply rewritten as

$$(-\rho_G \overline{\tilde{U} \cdot \tilde{V}})_{up} = c \frac{\rho_G U_r u_p}{h_a u_c} \sqrt{(h - h_m)^2} \cdot \sqrt{v_{uc}^2}. \quad [23]$$

Finally, the interfacial shear stress is expressed using [16] and [23]:

$$\tau_i(U_\infty) = \gamma \cdot \tau_{sw}(U_r) + c \frac{\rho_G U_r u_p}{h_a u_c} \sqrt{(h - h_m)^2} \cdot \sqrt{v_{uc}^2}. \quad [24]$$

In the above equation, the interfacial shear stress is different from the rough wall surface as a consequence of the increased interfacial area and the turbulent shear stress due to the wave motion.

5. COMPARISON WITH THE EXPERIMENTAL DATA

Figures 8(a, b) show the variation of the interfacial shear stress along the effective gas velocity U_r for the horizontal and vertical films. The interfacial shear stress at the horizontal film, with low film Reynolds number, is nearly same as the wall shear stress. This is because the interface is very smooth and the wave motion very small. Figures 9(a, b) show the turbulent shear stress due to the wave motion, expressed $\tau_i - \gamma \cdot \tau_{sw}(U_r)$ of [14], for the horizontal and vertical flows. The ratios of the interfacial area to its base area γ are taken from the experimental data of Kang & Kim (1992b). The values of γ are nearly unity, as discussed in the previous section. The turbulent shear stress by the wave motion is 30% of the wall shear stress of the single phase for the large air velocity

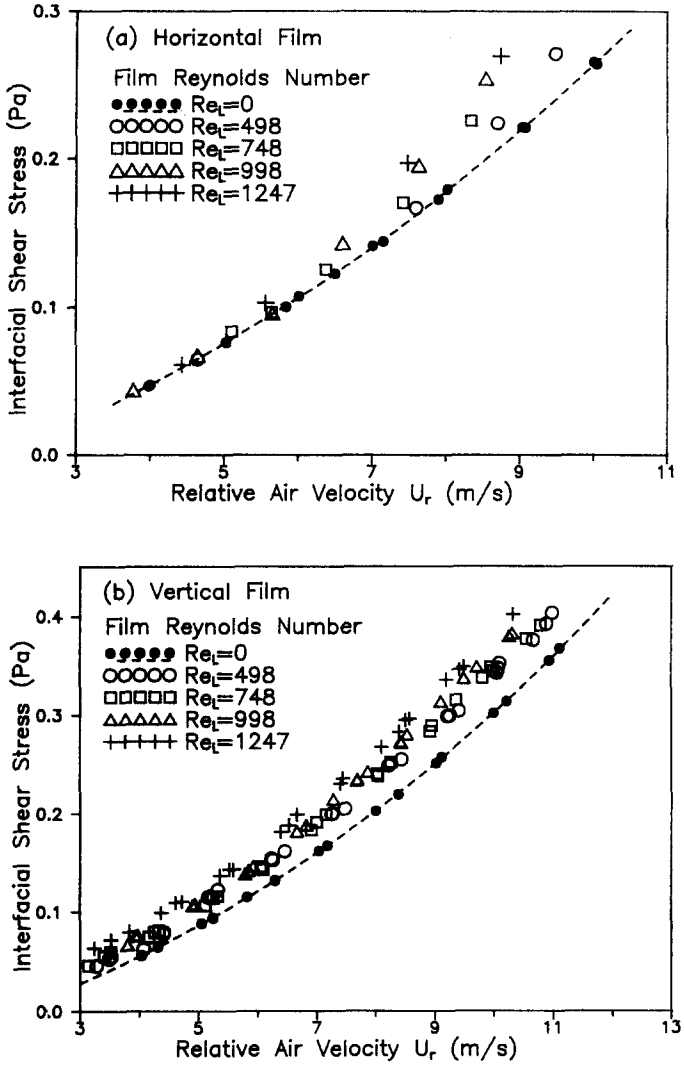

Figure 8. Interfacial shear stress at the (a) horizontal and (b) vertical films.

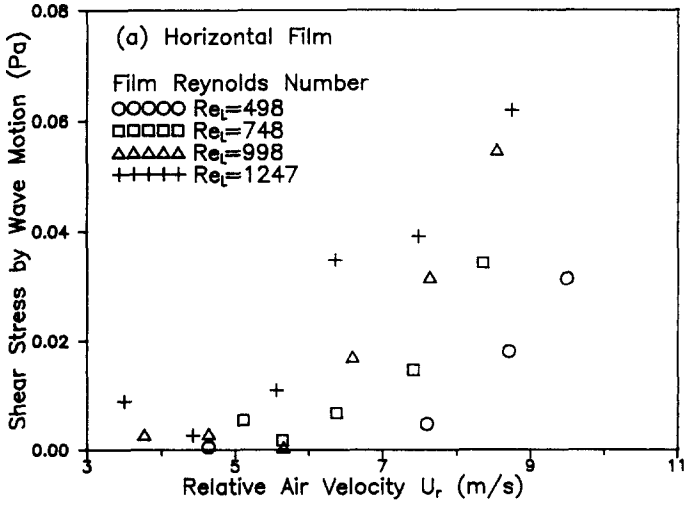

Figure 9—*continued opposite.*

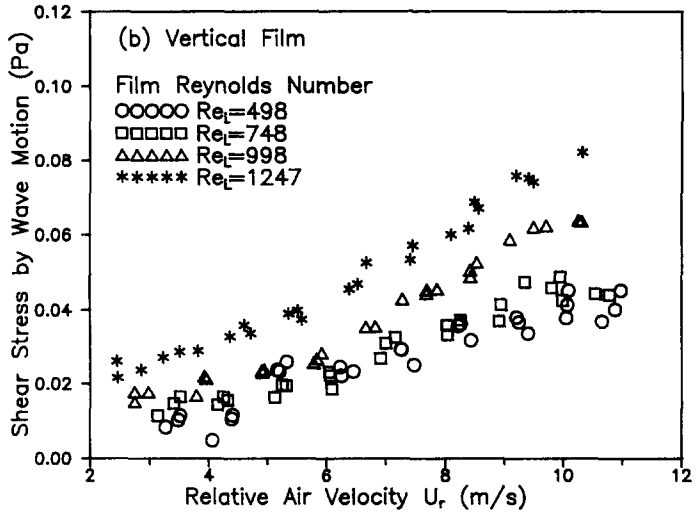

Figure 9. Shear stress due to the wave motion at the (a) horizontal and (b) vertical films.

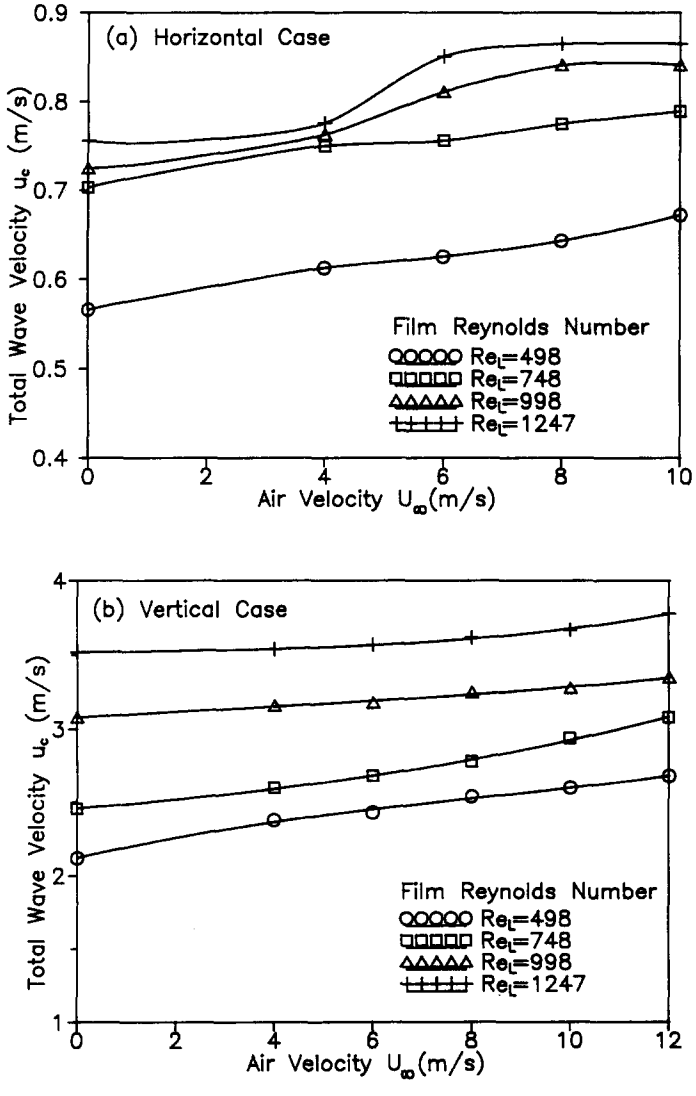

Figure 10. Total flow directional wave velocity u_c at the (a) horizontal and (b) vertical films.

Table 2. Comparison of the calculated interface velocity u_p with the photographic method for the vertical film

Re_L	Calculated velocity (m/s), A	Measured velocity (m/s), B	Error (%) $(A/B-1)100$
498	0.84	0.81	+3
748	1.04	0.97	+7
998	1.25	1.26	−1
1247	1.48	1.40	+6

($U_r \sim 10$ m/s) in this experiment. The shear stress from the wave motion depends on the air velocity and the water flow rate, but seems to be more dependent on the water flow rate in the vertical film.

The flow directional wave velocity at the interface u_p of [8] is checked by the photographic method of measuring the travel distance of a floating particle on the interface during the exposure time. The result agrees with the calculated interface velocities within 10%, as shown in table 2. The total wave velocities u_c of [7] are shown in figures 10(a, b). The wave velocity u_c is mainly changed by the film flow rate. The jump of u_c in figure 10(a) at $Re_L = 748$ is due to the transition of the two-dimensional wave to a three-dimensional wave. The ratio of the total wave velocity u_c to the bulk film velocity $\langle u \rangle$, which has been discussed by many researchers, is also very important here, in the expression [24] of the interfacial shear stress. The measured ratio for the vertical film is compared with the previous theoretical and experimental data in figure 11. The present experimental data are presented with the values predicted by the theories of Kapitza (1964), Massot *et al.* (1966) and Ishihara *et al.* (1961). The experimental data of Chu & Dukler (1975) and Takahama & Kato (1980) are lower than any theoretical values. This is believed to be mainly due to their film thickness measurement which has a rough spatial resolution, as discussed by Kang & Kim (1992). Therefore, they measured only the large waves, and lost the small waves in the multi-components of the vertical film. Actually, the wavelength in their measurement seems to be 10 times larger than the wavelength of the wave shape shown by their photographs.

The normal interface velocities $\sqrt{v_{uc}^2}$ of [11a, b] are shown in figures 12(a, b) for the horizontal and vertical films. The trend of $\sqrt{v_{uc}^2}$ is roughly similar to that of u_c.

Figure 13 shows the variation of $\tau_i - \gamma \cdot \tau_{sw}(U_r)$ against the $(\rho_G U_r u_p)/(h_a u_c)\sqrt{(h-h_m)^2} \cdot \sqrt{v_{uc}^2}$ of [23] in the horizontal and vertical flows. The coefficient c of [24] is the slope in figure 13, and is estimated at about 0.55 for both the horizontal and vertical films. The dispersion of the data may be due to experimental error, but they show a similar trend. Figure 14 shows the comparison of the calculated interfacial shear stress with the measured shear stress with $c = 0.55$. The calculated data agree well with the measured data for a wide variety of interfacial shapes of the horizontal and vertical films, for both the air and water flow rates.

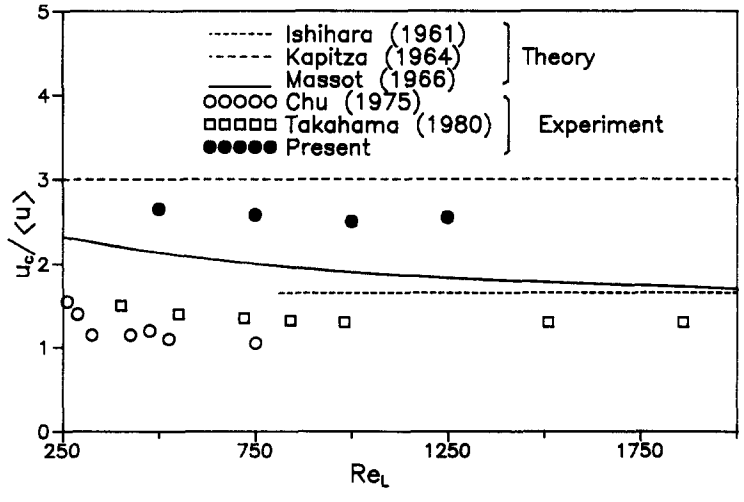

Figure 11. Comparison of the velocity ratio $u_c/\langle u \rangle$ with other works.

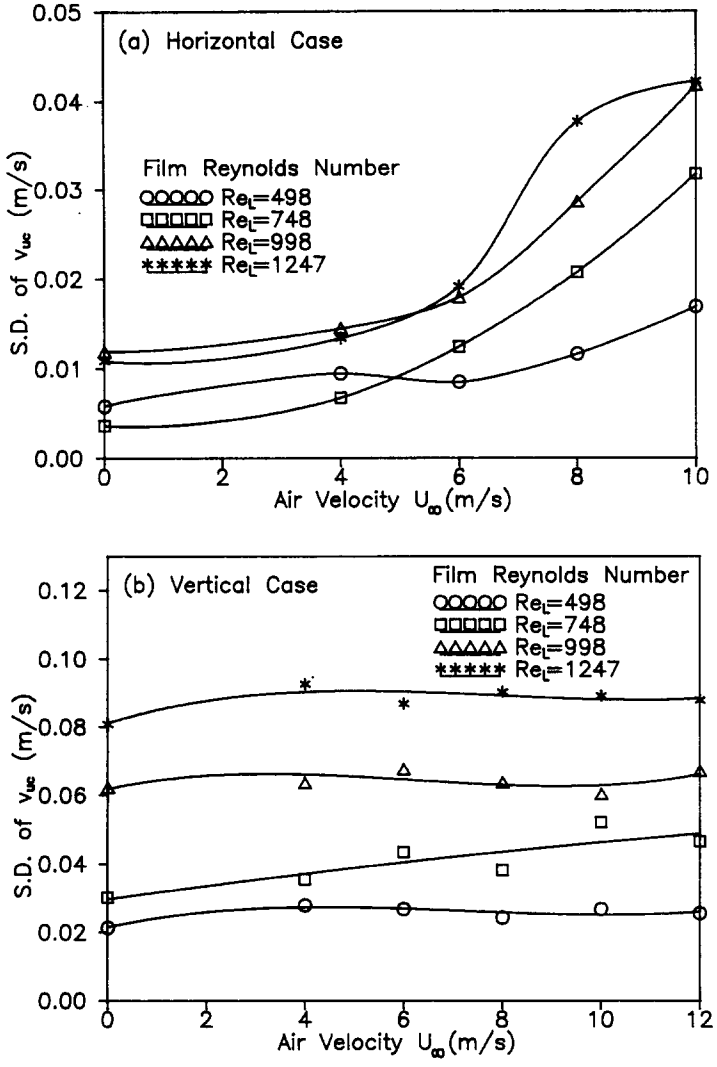

Figure 12. Standard deviation of the normal directional wave velocity v_{uc} at the (a) horizontal and (b) vertical films.

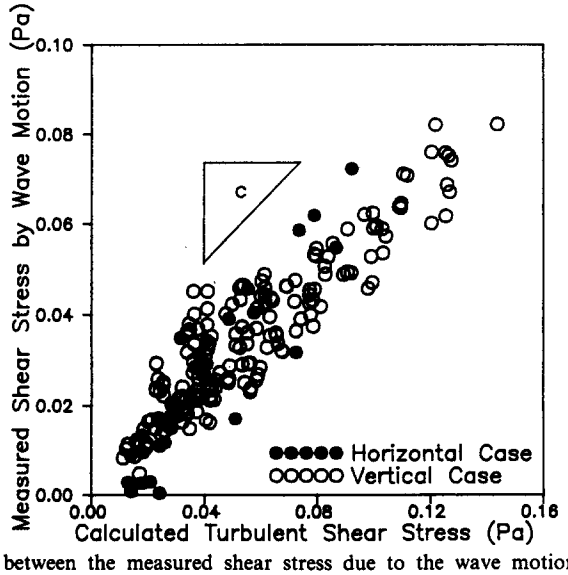

Figure 13. Relation between the measured shear stress due to the wave motion and the calculated turbulent shear stress.

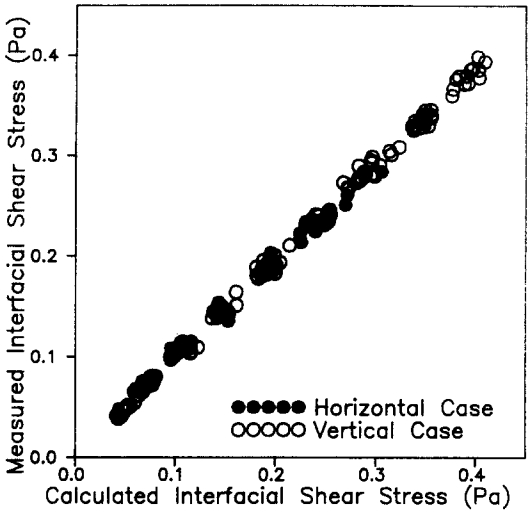

Figure 14. Comparison of the measured and calculated interfacial shear stress.

6. CONCLUSION

A model is developed to explain the interfacial shear stress using the normal velocity components of the interface and the effective gas velocity. It is based on the phenomenon itself in the wavy interface. The shear stress is considered as the summation of the shear stress exerted on the smooth wall surface and the shear stress due to the wave motion. The normal wave velocities measured at a fixed point show no correlation with the film thickness, but those measured in terms of moving coordinates have a negative correlation. Assuming a simple relation between the gas velocity near the interface and the film thickness, the turbulent shear stress due to the wave motion is expressed using the normal interfacial velocity and the effective gas velocity. The model agrees well with the experimental data for a wide range of horizontal and vertical stratified flows. This model will be applicable to the moderate range of stratified flow in which the flow separation near the wave is weak. This work focuses on concurrent stratified flow, but would also be applicable to countercurrent flow with some modifications. The model is, however, not in explicit form without knowledge of the interface shape and velocity in the flow condition. To improve the model for the transport phenomena in the interface, experimental data for the precise gas velocity are needed.

Acknowledgements—This work was performed with the support of the Korea Science & Engineering Foundation and the Advanced Fluids Engineering Research Center. The authors are grateful for this financial support.

REFERENCES

AKAI, M., INOUE, A. & AOKI, S. 1977 Structure of a co-current stratified two-phase flow with wavy interface. *Theor. Appl. Mech.* **25,** 445–456.

CHANG, P. C., PLATE, E. J. & HIDY, G. M. 1971 Turbulent air flow over the dominant component of wind-generated water waves. *J. Fluid Mech.* **47,** 183–208.

CHU, K. L. & DUKLER, A. E. 1974 Statistical characteristics of thin, wavy film—II. Studies of the substrate and its wave structure. *AIChE Jl* **20,** 695–706.

CHU, K. L. & DUKLER, A. E. 1975 Statistical characteristics of thin, wavy films—III. Structure of the large waves and their resistance to gas flow. *AIChE Jl* **21,** 583–593.

FUKANO, T., ITO, A., ODAWARA, H., KURIWAKI, T. & TAKAMATSU, Y. 1985 Liquid films concurrently with air in horizontal duct (5th report, shear stress at gas–liquid interface). *Trans. JSME* **51,** 494–502.

HAGIWARA, Y., ESMAEILZADEH, E., TSUTSUI, H. & SUZUKI, K. 1989 Simultaneous measurement of liquid film thickness, wall shear stress and gas flow turbulence of horizontal wavy two-phase flow. *Int. J. Multiphase Flow* **15,** 421–431.

HANSTOCK, W. H. & HANRATTY, T. J. 1976 The interfacial drag and the height of the wall layer in annular flows. *AIChE Jl* **22,** 990–1000.

ISHIHARA, T., IWAGAK, Y. & IWASA, Y. 1961 Discussion on roll waves and slug flows in inclined open channels. *Trans. Am. Soc. Civ. Engrs* **126,** 548.

KANG, H. C. & KIM, M. H. 1992a The development of flush-wire probe and calibration technique for measuring liquid film thickness. *Int. J. Multiphase Flow* **18,** 423–438.

KANG, H. C. & KIM, M. H. 1992b Measurement of three-dimensional wave form and interfacial area in an air–water stratified flow. *Nucl. Engng Des.* **136,** 347–360.

KAPITZA, P. L. 1964 Wave flow of thin layers of a viscous fluid. In *Collected Papers of P. L. Kapitza,* Vol. 2, pp. 662–713. Macmillan, New York.

KARAPANTSIOS, T. D. & KARABELAS, A. J. 1990 Surface characteristics of roll waves on free falling films. *Int. J. Multiphase Flow* **16,** 835–852.

KIM, H. J. 1983 Local properties of countercurrent stratified steam–water flow. Ph.D. Thesis, Northwestern Univ., Evanston, IL.

KOWALSKI, J. E. 1987 Wall and interfacial shear stress in stratified flow in a horizontal pipe. *AIChE Jl* **33,** 274–281.

LEVY, S. & HEALZER, J. M. 1981 Application of mixing length theory to wavy turbulent liquid–gas interface. *J. Heat Transfer* **103,** 492–501.

LILLELEHT, L. U. & HANRATTY, T. J. 1961 Relation of interfacial shear stress to the wave height for concurrent air–water flow. *AIChE Jl* **7,** 548–550.

LOCKHART, R. W. & MARTINELLI, R. C. 1949 Proposed correlation of data for isothermal two-phase, two-component flow in pipes. *Chem. Engng Prog.* **45,** 39–48.

MASSOT, C., IRANI, F. & LIGHTFOOT, E. N. 1966 Modified description of wave motion in a falling film. *AIChE Jl* **12,** 445–455.

PORTALSKI, S. & CLEGG, A. J. 1971 Interfacial area increase in rippled film flow on wetted wall columns. *Chem. Engng Sci.* **26,** 773–784.

PORTALSKI, S. & CLEGG, A. J. 1972 An experimental study of wave inception on falling liquid films. *Chem. Engng Sci.* **27,** 1257–1265.

SALAZAR, R. P. & MARSCHALL, E. 1978 Time-average local thickness measurement in falling liquid film flow. *Int. J. Multiphase Flow* **4,** 405–412.

SCHLICHTING, H. 1962 *Boundary Layer Theory,* p. 583. McGraw-Hill, New York.

TAKAHAMA, H. & KATO, S. 1980 Longitudinal flow characteristics of vertically falling liquid films without concurrent gas flow. *Int J. Multiphase Flow* **6,** 203–215.

WALLIS, G. B. 1969 *One-dimensional Two-phase Flow,* pp. 320–321. McGraw-Hill, New York.